

## CLEAVAGE AND THE IDENTIFICATION OF MINERALS

G. A. WOLFF\* AND J. D. BRODER,\* *U. S. Army Signal Research and Development Laboratory, Fort Monmouth, New Jersey.*

### ABSTRACT

"Mechanical etching" of substances gives a characteristic pattern that can serve as a means of identifying unknown minerals and other crystalline materials. The surfaces of single crystals can be ground with coarse abrasives in several ways; the microcleavage pits obtained can then be investigated by the light figure method. Sharp and diffuse spots and zonal reflections make up the pattern observed. The spots correspond to plane cleavages (macrocleavage) and the zones correspond to cylindrically curved microcleavages. There is always a center of symmetry introduced into the pattern, because in cleavage and microcleavage, the two newly created surfaces match.

Minerals and synthesized materials of various kinds have been investigated, and their patterns recorded. These patterns are arranged according to their structural relationship; similar patterns have been found for members of identical structure groups. Charts of these patterns, when arranged according to crystal systems and structures, will aid in the identification of unknown crystalline materials. Among the groups investigated were pyrite, marcasite, sphalerite, wurtzite, barite, halite, chrysolite and other structure groups.

Cleavage has been used since the beginning of the study of mineralogy to characterize minerals. Many minerals have been identified by their cleavage habit, i.e., "rhombohedral" for calcite; "cubic" for halite, and so on. Yet, the majority of mineral specimens are identified mainly from their natural habit, or from the results of chemical etching and/or from chemical and other analyses. In these cases, cleavage serves only as an auxiliary method of identification, or merely confirms the results. The reason for this is that reported cleavage data are often ambiguous. Differences among cleavage data have been reported by several authors. There are instances where different cleavages are shown for the same material obtained from different geographical locations. Dana (1) reports that stannite crystals from Cornwall show (110) and (001) cleavage, while stannite crystals from Bolivia show no cleavage. For this mineral, as for others, it has been suspected that the "cleavage" is caused by "parting"; and finally there are instances where, under the heading "cleavage" only fracture is reported and described in general terms as "conchoidal," "sub-conchoidal" or "hackly." This lack of reliability of the cleavage data has relegated it to a minor means of identifying minerals. An attempt has been made by Seaman (2) and Tertsch (3) to utilize cleavage as a means of classifying minerals. Though this work is an extensive collection of cleavage and habit data, there is little or sometimes no correlation apparent among the observed cleavages of one mineral and other min-

\* Present address: The Harshaw Chemical Company, Solid State Research, Cleveland 6, Ohio.

erals structurally related to it. Initially there was rapid progress toward an understanding of the principles of cleavage but a comprehensive interpretation of the data is still lacking.

Generally speaking, the study of habit and etch patterns is a successful method of identifying minerals because many planes are to be observed in growth and in etching. This method has a disadvantage, however, since each growth matrix and etch solution results in different growth or etch-pit habit. For successful identification, the different habit types and/or growth and etch solutions must be known. It may be, therefore, that microcleavage will provide a rapid and efficient means of identification.

#### "MICROCLEAVAGE" AND MINERAL IDENTIFICATION

Whereas cleavage, or "macrocleavage" refers to a separation of a crystal parallel to a crystal plane, "microcleavage" refers to the separation of a crystal parallel to crystallographic directions or zones which represent important atomic arrays (4) (PBC vector (5) Fig. 1). Where two or more microcleavage zones meet, macrocleavage occurs. A method utilizing both types of cleavage has the following advantages in identifying minerals: (1) Any particular material, of a specific structure, shows only one specific microcleavage pattern which, for all practical purposes, is independent of small amounts of impurities, temperature and cleaving technique; (2) In chemical etching, a suitable etchant must be found. This is a matter of trial and error in most instances. The natural habit may help to identify the substance, but for substances having many known habits it is a tedious process. Obviously, if the habit is not visible, the problem becomes a difficult one; (3) Within a group of similar structure, the cleavage should be similar, with possible minor variations. It will be shown in the text, and in the tables that this holds true for microcleavage of substances with identical structure but dissimilar chemical properties, for example  $\text{KMnO}_4$  and  $\text{BaSO}_4$ , and  $\text{CaCO}_3$  and  $\text{NaNO}_3$ ; (4) Since a center of symmetry is introduced in the patterns, the number of symmetry classes that can be identified is reduced to eleven.

The statement given under (4) is the ideal case. Deviations from this rule are observed and an elaboration should be given. For a substance with a known crystal class, the corresponding class to be observed in microcleavage is predetermined. Yet, there are cases to be expected where the observed symmetry is higher. Let us consider, for example,  $\text{NaClO}_3$  (class 23), hauerite ( $\text{MnS}_2$ ),  $\text{Pb}(\text{NO}_3)_2$ ,  $\text{Ba}(\text{NO}_3)_2$  (class  $2/m\bar{3}$ ). The supposed cations and anionic groups are centered in positions which correspond to the  $\text{Na}^+$  and  $\text{Cl}^-$  positions in  $\text{NaCl}$ . When the interionic distance is large as compared to the intraionic distance, then the interaction between the cations and "anions" is such that no complexity is introduced

between them. The situation is then similar to that in NaCl. In other words, the interaction of the cation and anionic group is non-directional and non-specific; therefore, instead of the expected  $2/m\bar{3}$  symmetry, the  $4/m\bar{3}$  symmetry of the NaCl structure is observed. Correspondingly, cubic symmetry may be observed rather than tetragonal symmetry (as in BaTiO<sub>3</sub>) etc. Multiple twinning may also lead to a higher order of symmetry and thus deceive the observer. Arsenopyrite (FeAsS) for instance, which is actually monoclinic with  $\beta=90^\circ$ , shows orthorhombic symmetry (6). In addition, there are cases, as in tellurium and cinnabar (32), where no decision can be made between the symmetry classes  $\bar{3}2/m$  and  $6/m2/m2/m$  because the macrocleavage and microcleavage planes are in special positions (*i.e.* symmetry positions).

#### THE INTERPRETATION OF MICROCLEAVAGE; MICROCLEAVAGE AND PBC VECTORS

In the investigation of microcleavage, it is important to determine the crystallographic zones of microcleavage. These zones represent atomic or ionic arrays of strong bonding at the surface ("PBC Vectors"). The interpretation of the results yields useful information of surface structure and bonding. Since it applies only indirectly in the identification of crystalline materials by their microcleavage patterns, only a short discussion follows. Each plane of a crystal of any given structure has a specific value of surface free energy,  $E$ . The specific surface free energy plots of a crystal, in spherical coordinates, show maxima, cusp valleys, and cusps arranged according to the symmetry of the crystal structure. The cusp valleys and the cusps are of importance; the valleys correspond to bond arrays and the cusps correspond to the intersection of two or more such arrays. In a Wulff's Plot (7), they correspond to edges and planes, respectively. The total area,  $S$ , of any particular crystallographic plane of a crystal decreases rapidly with increasing surface free energy  $E$  for growth and etch habits; as a first approximation,  $S$ , for microcleavage is proportional to  $e^{-BE}$  where  $B$  is a constant. Since for parallel light of uniform light flux, as is employed in the light figure method described below, the sum of the reflected light is proportional to  $S$ , the growth, etch and cleavage habit can be determined. As a matter of fact, this is the only general method of determining the cleavage habit when more than one cleavage plane is observed. The following can occur: (1) when the valleys are "complete," that is, cover an angle of  $360^\circ$ , the atoms lie either in one straight line, as in the simple cubic structure, in  $[001]$  (Fig. 2a), or they are composed of zig-zag arrays of atoms which are at least triple ( $[0001]$  in wurtzite). (2) Any zig-zag array is composed of at least two vectors, and as such results in an "incomplete" valley, that is, a surface free energy minimum valley covering a fraction of  $360^\circ$  (Fig. 2b). (3) The

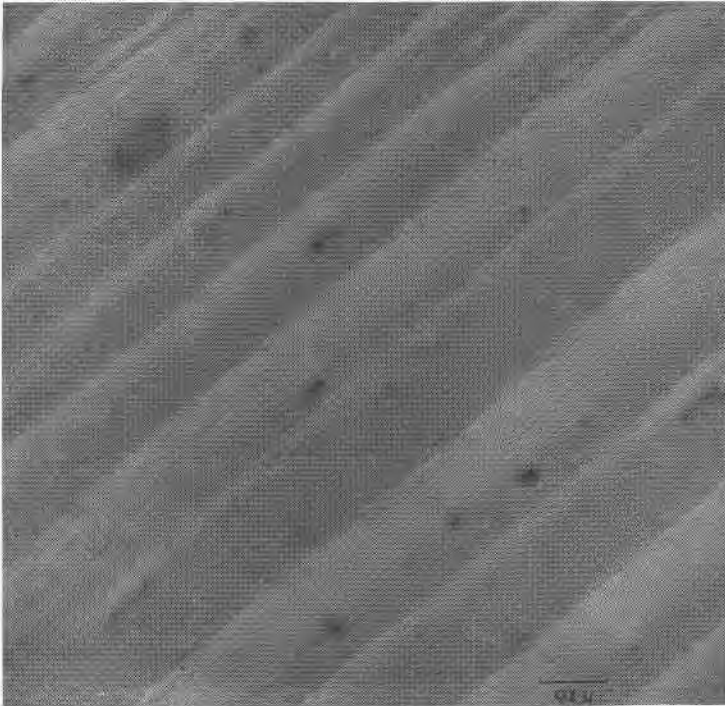


FIG. 1. Electron micrograph of the surface of a “(110) cleavage” in diamond showing a system of troughs parallel to [110]. The cylindrically curved portions of the troughs represent  $hhl$  planes with  $h > l$ ; the lighter and darker portions correspond to (111) and  $(\bar{1}11)$  cleavage planes, respectively.

same is sometimes true for PBC vectors composed of two different bond vectors ( $V_1, V_2$ ; *e.g.* Sb and Te). It is characteristic of this type that when the ratio of the two bond strengths exceeds a critical value, one of the valleys disappears, giving way to another. (4) The valley does not coincide with a zone parallel to a PBC vector derived from the crystalline structure. In this case, the PBC vectors are present only at the surface, where, during the separation of the two planes during the cleavage process, the atoms move into positions energetically superior to the positions of the ideal unchanged surface. Thus, a new PBC vector appears which is not present in the bulk structure and therefore, the surface energy is lowered. The vector is mostly of the zig-zag type. (5) New PBC vectors can also appear when adsorption takes place. They determine the growth, solution and equilibrium forms, but since adsorption takes place only after the cleavage planes have formed, for cleavage this effect can be disregarded.

It can be shown that the microcleavage pattern is closely related to

the surface energy plot (Wulff's Plot) and the PBC vector diagram of the corresponding structure. The following examples where this relationship was studied and found to hold are: diamond, arsenolite, senarmontite, cuprite, fluorite, magnesite and marcasite. The ideal pattern, as predicted on this basis, is also shown by GaSb and other materials of the B3 structure type, with their ionic character reflected in the appearance of (011)

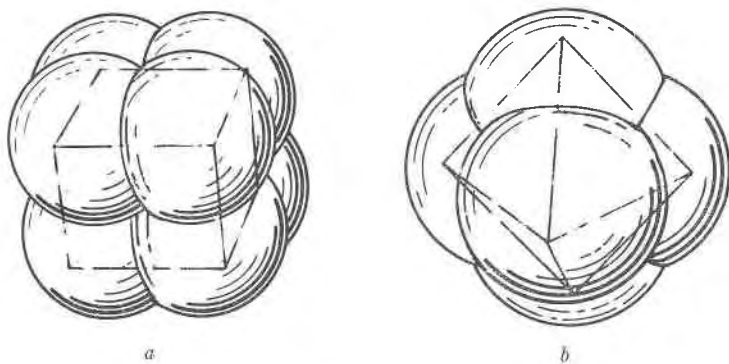


FIG. 2a. Surface free energy plot of a crystal of simple cubic structure in spherical coordinates. Only nearest neighbor interaction is taken into account. Each cusp corresponds to an equilibrium plane (001); each valley connecting the cusps correspondingly represents an edge. This edge is [100] and is the common boundary to two adjacent (001) planes. The valleys are "complete," i.e. they can be traced  $360^\circ$  from cusp to cusp around the plot along one zone. A complete valley corresponds to a straight array of atoms. The equilibrium form (001) is inscribed.

FIG. 2b. Surface free energy plot for a crystal of diamond structure in spherical coordinates. Only nearest neighbor interaction is taken into account. The cusps correspond to (111) planes and the valleys connecting them correspond to [011] edges which are common to two neighboring (111) planes. The valleys are "incomplete" *i.e.*, they cannot be traced  $360^\circ$  around the plot. An incomplete valley corresponds to a zig-zag array. The equilibrium form (111) is inscribed.

cleavage planes (4). The (011) cleavage of NaCl which appears in addition to the expected pattern is apparently caused by the combined action of microcleavage in [010] and glide in [011].

Prismatic microcleavage patterns reveals the chain structure of both tellurium and the related compound cinnabar.

#### MECHANICAL ETCHING AND EXPERIMENTAL DETERMINATION OF MICROCLEAVAGE

Microcleavage may be observed when the crystals are "mechanically etched" (4). Mechanical etching can be described as follows: first, the material under investigation is cut roughly, or ground into spherical

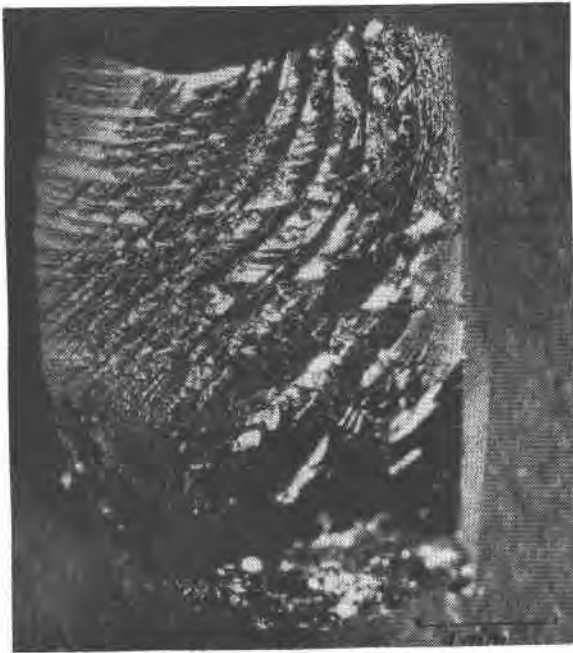


FIG. 3. Photomicrograph of fractured silicon surface showing two sets of stress wave patterns. No structural features are revealed in the light figure investigation.

shape. Next, it is subjected to a rough grinding process that can be carried out in any of the following ways: either the sphere is rolled under moderate pressure between two sheets of very coarse SiC paper, or it is rotated in a coarse SiC slurry, carried in a hollow pipe mounted on the shaft of a counter rotating motor, or it can be spun with SiC particles in a modified Bond Wheel (8). For materials which are as hard or harder than SiC, coarse diamond powder is used. For soft materials, or materials having predominantly metallic character, slipping is observed rather than cleavage. At low temperatures, metals or soft materials are more brittle and then are subject to the same laws of cleavage as brittle material at room temperature. When this type of etching is employed, a cleavage pattern is observed when the surface of the sphere is studied by the light figure method (9). The light figure apparatus consists of a point source of light, a collimating lens system mounted on an optical bench, and a modified goniometer. A screen is mounted so that the light which comes through a hole in the center of the screen impinges on the crystal mounted on the goniometer. The crystal is spherical in shape, of about the same size as the hole and this permits observation of the major portion of the

surface at one time. The advantage of this method over conventional goniometry is that zones can be observed with greater ease, and the differences in intensities can be seen with greater accuracy. This apparatus also permits the observer to make a photographic record of the cleavage pattern. By reducing the size of the hole to small diameters, ( $\sim 0.25$  mm.), the illuminated and reflecting area of the crystal can be reduced. Thus a polycrystalline sample can be scanned and evaluated, crystal for crystal, with respect to their orientation and to crystallographic differences for different areas of each single crystal. Multiple reflections can be discerned and eliminated by the difference in their rate and direction of motion on the screen, when compared with the rate and direction of motion of the primary reflections. The angular motion of the latter is  $2\alpha$  when the crystal in the goniometer is rotated by an angle of  $\alpha$ .

Various substances, both minerals and laboratory synthesized materials, have been investigated. Their patterns have been observed and recorded and arranged in charts according to structural relationships, so that they can serve as a method of identification.

















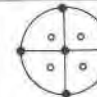








#### DISCUSSION OF THE PATTERNS

Table 1 compares the cleavage data as reported in Dana (1) with the stereographic projections of the observed cleavages. The reported cleavage is tabulated above the stereogram. It should be understood that the stereograms represent an idealized picture and do not show all the nuances that are actually observed. The spots represent reflections from individual planes, and the zones (unbroken lines) represent reflections from a whole series of planes lying along a particular direction. An attempt has been made to indicate the relative intensities of the reflections by the heaviness of the spots or zones. The open circles represent broad, diffuse reflections. It should be noted that cleavage zones are not mentioned directly in Dana. Their existence is recorded in the mention of the terms conchoidal, hackly, etc. In the majority of cases, there are indications that conchoidal fractures represent microcleavages of a complex nature. They are a combination of a number of micro- or macrocleavages parallel to one, or more, directions (a unifold infinite number, parallel to each direction). Visually, this is noticeable only in rare cases.

Generally, the more hackly the pattern, the more the fracture is determined by the action of shock waves and stress propagation rather than by structural aspects. The microscopic inspection of hackly fracture patterns in silicon, for instance, strikingly reveals the stress wave pattern Fig. 3.

The variation in appearance of the zones and the relative intensities of the reflections can also aid in the identification of crystalline materials.

TABLE 1. THE MICROCLEAVAGE PATTERNS OF MINERALS AND ARTIFICIAL SINGLE CRYSTAL MATERIALS RECORDED AS STEREOGRAPHIC PROJECTIONS. THE CHEMICAL FORMULA AND THE CLEAVAGE AS REPORTED IN DANA ARE ALSO GIVEN

DIAMOND	ARSENOLITE	SILICON	GREY TIN	GoSb
C	As <sub>4</sub> O <sub>6</sub>	Si	α-Sn	
III PERFECT	III			
	 SIMILAR PATTERN FOR SENARMONTITE	 SIMILAR PATTERN FOR Ge		 SIMILAR PATTERN FOR InAs, InSb
AlSb	SPHALERITE	TIEMANNITE	COLORADOITE	CUPRITE
	ZnS	HgSe	HgTe	Cu <sub>2</sub> O
	OII PERFECT	NONE	NONE	III INTERRUPTED OOI RARE
	 SIMILAR PATTERN FOR GoP, AlP, AlAs, ZnSe, CuI			
FLUORITE	AuGa <sub>2</sub>	HALITE	PERICLASE	GALENA
CaF <sub>2</sub>		NaCl	MgO	PbS
III PERFECT OOI SOMETIMES		OOI PERFECT	OOI PERFECT III IMPERFECT OII PARTING	OOI EASY & PERFECT III PARTING
	 SIMILAR PATT. FOR AuIn <sub>2</sub>	 SIMILAR PATT FOR LiF, KBr		 SIMILAR PATT FOR PbTe, SnSe
NaClO <sub>3</sub>	HAUERITE	PYRITE	COBALTITE	ULLMANNITE
	MnS <sub>2</sub>	FeS <sub>2</sub>	CoAsS	NiSbS
	OOI PERFECT	OOI, OII, III INDISTINCT	OOI PERFECT	OOI PERFECT
				
Pb(NO <sub>3</sub> ) <sub>2</sub>	Ba(NO <sub>3</sub> ) <sub>2</sub>	MAGNETITE	SPINEL	FRANKLINITE
		Fe <sub>3</sub> O <sub>4</sub>	MgAl <sub>2</sub> O <sub>4</sub>	ZnFe <sub>2</sub> O <sub>4</sub>
		III, OOI, OII, I38 PARTING	III INDISTINCT "SEPARATION" PLANE	III PARTING
				

CUBIC



TABLE 1 (Continued)

	ZIRCON $ZrSiO_4$	KDP $KH_2PO_4$	ADP $NH_4H_2PO_4$	SCHEELITE $CaWO_4$	WULFENITE $PbMoO_4$
	110 IMPERFECT 111 INDISTINCT			101 DISTINCT 112 INTERRUPTED 001 INDISTINCT	011 DISTINCT 001 } 013 } INDISTINCT
TETRAGONAL	RUTILE $TiO_2$	CASSITERITE $SnO_2$	ANATASE $TiO_2$	HAUSMANNITE $Mn_3O_4$	CHALCOPYRITE $CuFeS_2$
	110 DISTINCT 100 LESS SO 111 IN TRACES	100 IMPERFECT 110 INDISTINCT 111 OR 011 PARTING	001 } PERFECT 011 }	001 NEAR PERF. 112 } INDISTINCT 011 }	011 SOMETIMES DISTINCT
	BARITE $BaSO_4$	CELESTITE $SrSO_4$	ANGLESITE $PbSO_4$	KMnO <sub>4</sub>	ANHYDRITE $CaSO_4$
	001 PERFECT 210 LESS PERF. 010 IMPERFECT	001 PERFECT 210 GOOD 010 POOR	001 GOOD 210 DISTINCT 010 TRACES	*	010 PERFECT 100 NEAR PERF. 001 GOOD
	CHRYSOLITE $(Mg, Fe)_2SiO_4$	FAYALITE $Fe_2SiO_4$	TEPHROITE $Mn_2SiO_4$	CHRYSOBERYL $BeAl_2O_4$	TRIPHYLITE $LiFe(PO_4)$
	010 DISTINCT 100 LESS SO	010 DISTINCT 100 LESS SO	DISTINCT IN TWO DIRECTIONS AT RIGHT ANGLES	110 DISTINCT 010 IMPERFECT 001 POOR	100 NEAR PERF. 010 IMPERFECT 011 INTERRUPTED
RHOMBIC	CERUSSITE $PbCO_3$	STIBNITE $Sb_2S_3$	BISMUTHINITE $Bi_2S_3$	MARCASITE $FeS_2$	ENARGITE $Cu_3AsS_4$
	110 & 021 DIST. 010 & 012 IN TRACES	010 PERFECT & EASY 100, 110 IMPERF.	010 PERFECT & EASY 100, 110 IMPERF.	101 DISTINCT 110 TRACES	110 PERFECT 100, 010 DIST. 001 INDISTINCT

TABLE 1 (Continued)

	QUARTZ	BERLINITE	CORUNDUM	HEMATITE	Cr <sub>2</sub> O <sub>3</sub>
	SiO <sub>2</sub>	AlPO <sub>4</sub>	Al <sub>2</sub> O <sub>3</sub>	Fe <sub>2</sub> O <sub>3</sub>	
	101̄1, 101̄0, 011̄1 0001 DIFFICULT	NONE	NONE 0001 011̄2 } PARTING	NONE 0001 011̄2 } PARTING	
			SIMILAR PATTERN FOR RUBY (99% Al <sub>2</sub> O <sub>3</sub> ; 2% Cr <sub>2</sub> O <sub>3</sub> )		
	WURTZITE	GREENOCKITE	ZINCITE	CARBORUNDUM	TELLURIUM
	ZnS	CdS	ZnO	SiC	Te
	112̄0 EASY 0001 DIFFICULT	112̄2 DISTINCT 0001 IMPERFECT	101̄0 PERFECT 0001 PARTING	CONCHOIDAL FRACTURE	101̄0 PERFECT 0001 IMPERFECT
		SIMILAR PATTERN FOR CdSe		SIMILAR PATTERN FOR Acl	
HEXAGONAL	CALCITE	MAGNESITE	SIDERITE	RHODOCHROSITE	DOLOMITE
	CaCO <sub>3</sub>	MgCO <sub>3</sub>	FeCO <sub>3</sub>	MnCO <sub>3</sub>	CaMg(CO <sub>3</sub> ) <sub>2</sub>
	101̄1 PERFECT 0001 011̄2 } PARTING	101̄1 PERFECT	101̄1 PERFECT	101̄1 PERFECT 011̄2 PARTING	101̄1 PERFECT 0221 PARTING SOMETIMES
	WILLEMITE	PHENACITE	PROUSTITE		
	Zn <sub>2</sub> SiO <sub>4</sub>	Be <sub>2</sub> SiO <sub>4</sub>	Ag <sub>3</sub> AsS <sub>3</sub>		
	0001 MORSENET 112̄0 N J 0001 DIFF. N J	112̄0 DISTINCT 101̄1 IMPERFECT	101̄1 DISTINCT		
	CROCOITE	SPODUMENE	WOLLASTONITE	ARSENOPYRITE	MANGANITE
	PbCrO <sub>4</sub>	LiAl(SiO <sub>3</sub> ) <sub>2</sub>	CaSiO <sub>3</sub>	FeAsS	MnO(OH)
	110 DISTINCT 001, 100 INDIST.	110 PERFECT	100, 001 PERF. 101 LESS SO	101 DISTINCT 010 TRACES	010 VERY PERF. 110, 001 LESS PERFECT
MONOCLINIC					

### *Cubic System*

In Dana, (111) macrocleavage is reported for diamond, arsenolite and senarmontite, but no mention is made of the zones as shown in the stereogram. Also, note that Si, Ge and  $\alpha$ -Sn, which crystallize with the diamond structure have a zonal pattern different from that of diamond. This has been explained in previous papers by the authors and by others (4, 10) and is the result of surface deformation.

Halite and periclase are both structurally and chemically similar and both are strongly ionic crystals. The same cleavage would be expected to be observed for both, yet in Dana, NaCl is reported as having (001) macrocleavage and periclase (001), (111) and "(011) parting." It is our belief that the cleavages of the two materials should be consistent and no (111) macrocleavage should be found because of the strongly ionic character of the substances. The same reasoning would account for the fact that no (111) macrocleavage is to be observed in PbS. Furthermore, the reported (011) parting as sometimes occurring in periclase is also dubious since it is consistently revealed in our samples. It should also be noted that (011) appears in NaCl; though not reported in Dana, it has been reported by others (3).

AuGa<sub>2</sub> and AuIn<sub>2</sub>, having the same structure as CaF<sub>2</sub>, show additional zonal structure.

Artificial HgSe and HgTe have patterns consistent with their structural group but differ from those of the III-V compounds (4).

Hauerite, cobaltite, Pb(NO<sub>3</sub>)<sub>2</sub> and Ba(NO<sub>3</sub>)<sub>2</sub> show a higher order of symmetry than pyrite, as explained in the text. Gersdorffite, which has the same cleavage pattern as cobaltite, has not been included in the charts.

### *Tetragonal System*

Note the complex structure revealed by chalcopyrite in contrast to the reported (011) in Dana. Higher index planes were observed in ADP (NH<sub>4</sub>H<sub>2</sub>PO<sub>4</sub>) that could not be indexed; the "(112)" in rutile is an approximation.

Pyrolusite and stannite have been investigated, though not recorded on the chart; pyrolusite showing a continuous prismatic microcleavage reflection and stannite shows microcleavage between (001) and (012), between (012) and (112) and between (112) and (110). Distinct cleavage found for (012), (112) and (001) in order of increasing intensity.

### *Orthorhombic System*

Barite and KMnO<sub>4</sub>, both chemically different, yet structurally related, give very similar patterns. Barite also has a microcleavage pattern that differs from the other sulfates studied.

Glaucodot and loellingite, not shown on the charts, reveal (010) and (101) cleavage and a strong zone between (101) and  $(\bar{1}01)$ . In addition, glaucodot shows (100) cleavage and a weak microcleavage zone between (100) and (101), while loellingite shows weak cleavage in (011) and weak microcleavage between (011) and (001). Laboratory grown specimens of sulfur crystals show (111) cleavage.

### *Hexagonal System*

ZnS, CdS and ZnO are structurally and chemically closely related, yet three different cleavages are reported in Dana. The stereograms reveal that all have basically the same cleavage. One group of CdS samples also consistently reveals a pyramidal macrocleavage which could not be explained.

Cinnabar has a cleavage pattern similar to that of Te except that the basal cleavage (0001) is not present.

Parting is mentioned for ZnO,  $\text{CaCO}_3$ ,  $\text{Fe}_2\text{O}_3$  and  $\text{Al}_2\text{O}_3$ . This implies a random observation of the particular plane, yet the plane (or planes) consistently appear as many tiny cleavage pits over the different, but equivalent, directions affected and should be considered as true cleavage planes.

Note the zones that appear in magnesite and siderite in addition to the planes, and the difference between these minerals and the other carbonates.

The following minerals are not listed on the charts: ilmenite ( $\text{FeTiO}_3$ ) exhibits (10 $\bar{1}$ 1) cleavage planes; millerite (NiS) shows a pattern very similar to that of calcite, however no zones run through the (10 $\bar{1}$ 1) spot;  $\text{NaN}_3$  shows a pattern identical to that of calcite.

### *Monoclinic System*

In addition to the reported cleavage planes for spodumene and wollastonite, other planes and zones have been found and are shown on the stereograms.

## CONCLUSION

In conclusion, this method of producing and observing cleavage offers a new tool for the mineralogist, not only for the identification of unknown minerals by their cleavage habit, as first attempted by Seaman (2) and Tertsch (3) but also as a means of a systematic and scientific investigation of the cleavage phenomena. An analysis of the cleavage patterns, together with a knowledge of the crystal structure can yield information concerning the type of bonding in the crystal. The ratio of ionic to covalent bonding in crystals with the sphalerite structure has been determined this way.

## ACKNOWLEDGMENTS

The authors would like to acknowledge the invaluable aid given them by Mr. D. Seaman of the Mineralogy Department of the American Museum of Natural History and Mr. R. Hesse of the Academy of Natural Sciences in Philadelphia, Dr. G. Switzer and Mr. P. E. Desautels of the U. S. National Museum in Washington, D. C., as well as others for supplying mineral and crystal specimens used in this work. Special thanks are due Mr. P. Bramhall of this Laboratory for growing  $\text{Ba}(\text{NO}_3)_2$ ,  $\text{Pb}(\text{NO}_3)_2$ ,  $\text{NaClO}_3$ , crystals and Mr. C. F. Cook of this Laboratory for the electron micrography. Thanks are also due to Drs. R. M. Denning of the University of Michigan and F. W. Leonhard of this Laboratory for stimulating discussions, and to Dr. S. B. Levin of this Laboratory for his interest in this work.

## REFERENCES

1. J. D. DANA, "The System of Mineralogy," 1944-1951, John Wiley & Sons, N. Y.
2. W. A. SEAMAN, "Mineral Classification," Michigan College of Mining and Technology, 4th Edition, 1935; K. Spiroff, "Seaman's Mineral Tables," The Michigan College of Mining and Technology Press, 1959.
3. H. TERTSCH, "Die Festigkeitserscheinungen der Kristalle," 1959, Springer, Vienna.
4. G. A. WOLFF AND J. D. BRODER, *Acta Cryst.* **12**, 313 (1959).
5. P. HARTMAN AND W. G. PERDOK, *Acta Cryst.* **8**, 49 (1955).
6. M. J. BUERGER, *Z. Krist.* **94**, 83 (1936).
7. G. WULFF, *Z. Krist.* **34**, 449 (1901).
8. W. L. BOND, *Rev. Sci. Instrum.* **22**, 344 (1951).
9. G. A. WOLFF, J. M. WILBUR, JR., AND J. C. CLARK, *Z. Elektrochem.* **61**, 101 (1957).
10. W. B. PEARSON AND G. A. WOLFF, *Faraday Soc. Discussions*, **28**, 142 (1959).

*Manuscript received March 2, 1960.*